

See discussions, stats, and author profiles for this publication at: <https://www.researchgate.net/publication/40032074>

# Time Dependent Sphere-to-Rod Growth of the Pluronic Micelles: Investigating the Role of Core and Corona Solvation in Determining the Micellar Growth Rate

ARTICLE in THE JOURNAL OF PHYSICAL CHEMISTRY B · NOVEMBER 2009

Impact Factor: 3.3 · DOI: 10.1021/jp9036974 · Source: PubMed

CITATIONS

24

READS

57

6 AUTHORS, INCLUDING:



**Yogesh Kadam**

Veer Narmad South Gujarat University

11 PUBLICATIONS 190 CITATIONS

SEE PROFILE



**Rajib Ganguly**

Bhabha Atomic Research Centre

61 PUBLICATIONS 918 CITATIONS

SEE PROFILE



**Vinod K Aswal**

Bhabha Atomic Research Centre

392 PUBLICATIONS 4,905 CITATIONS

SEE PROFILE



**Pratap Bahadur**

Veer Narmad South Gujarat University

179 PUBLICATIONS 3,636 CITATIONS

SEE PROFILE

## ARTICLES

## Time Dependent Sphere-to-Rod Growth of the Pluronic Micelles: Investigating the Role of Core and Corona Solvation in Determining the Micellar Growth Rate

Y. Kadam,<sup>†</sup> R. Ganguly,<sup>\*,‡</sup> M. Kumbhakar,<sup>§</sup> V. K. Aswal,<sup>||</sup> P. A. Hassan,<sup>‡</sup> and P. Bahadur<sup>†</sup>

Department of Chemistry, V.N. South Gujarat University, Surat 395007, Chemistry Division, Radiation & Photochemistry Division, Solid State Physics Division, Bhabha Atomic Research Center, Mumbai 400 085, India

Received: April 22, 2009; Revised Manuscript Received: October 9, 2009

The salt induced sphere-to-rod growth in the micelles of the PEO–PPO triblock copolymers, Pluronic P123 (EO<sub>20</sub>PO<sub>70</sub>PEO<sub>20</sub>) and Pluronic P103 (EO<sub>16</sub>PO<sub>61</sub>PEO<sub>16</sub>), has been studied by dynamic light scattering (DLS), viscometry, and small angle neutron scattering (SANS) techniques. The observed micellar growths are found to be time dependent and have a strong variation in their growth rate with changing anion type and copolymer composition. The rate of growth increases rather significantly with an increase in the water structure making abilities of the anions along the Hofmeister series in the order  $\text{Cl}^- < \text{F}^- < (\text{PO}_4)^{3-}$ . This has been attributed to an increasing ability of these ions to dehydrate the micellar corona, a factor that plays an important role in inducing sphere-to-rod shape transition of the micelles. The copolymer composition also has a significant influence on the micellar growth rate, as the P103 with a smaller molecular weight than P123 shows a significantly faster growth of its micelles under similar conditions. The observed time dependence in micellar growth in these systems has been attributed to a slow micellar restructuring process necessary to attain the equilibrium structure of the micelles. A remarkable improvement in the growth rate of the micelles, however, could be achieved in the presence of ethanol, a solvent that has affinity toward both the PPO and PEO blocks. Our spectroscopic studies suggest that the observed improvement in the micellar growth rate by ethanol is due to an accelerated restructuring process of the micelles in the presence of the solvated micellar core. These studies thus highlight the role of changing core and corona solvation characteristics of the pluronic micelles in determining their rearrangement and the growth rate, which is first of its kind in the aqueous pluronic system.

## Introduction

The polyethylene oxide–polypropylene oxide–polyethylene oxide (PEO–PPO–PEO) triblock copolymers have been the subject of interest of researchers for over two decades due to their wide range of applications and rich structural polymorphism.<sup>1–13</sup> In an aqueous medium, the self-assembling characteristics of these copolymers are determined primarily by strongly temperature dependent and differential solubility characteristics of their constituent blocks.<sup>10</sup> At low temperature, both the PPO and PEO blocks are soluble in water and the copolymer remains singly dissolved as unimers. At the critical micellar temperature (CMT), it starts forming micelles comprising a hydrophobic core containing the PPO blocks and a hydrated corona containing the PEO blocks.<sup>11–13</sup> Since the solubility of the PEO block decreases with an increase in temperature above the CMT, the micelles undergo restructuring to increase their aggregation number and core size, and to decrease their degree of hydration.<sup>11,14,15</sup> For some of the copolymers, such restructuring processes lead to a sphere-to-rod micellar shape change when

the size of the core becomes equal to the length of the stretched PPO chain.<sup>16,17</sup> At still higher temperature, large micellar clusters start forming, the concentration of which increases with an increase in temperature until the copolymer solution phase separates at the cloud point (CP).<sup>18–20</sup>

Recently, it has been shown by us that the aqueous P123 (EO<sub>20</sub>PO<sub>70</sub>PEO<sub>20</sub>) solutions show a slow and time dependent sphere-to-rod micellar growth on approaching their cloud points.<sup>21</sup> It has been suggested that a high molecular weight of the P123 slows down the micellar restructuring process necessary to attain the temperature dependent equilibrium structure of the micelles. The situation is even more complex in the presence of water structure making salts like NaCl, KCl, KF, etc., which are known to reduce the sphere-to-rod micellar growth temperature of the copolymer solutions down to room temperature.<sup>22–24</sup> It has been found that the presence of these salts leads to a partial conversion of the copolymer micelles from spherical to wormlike shape at room temperature, and the extent of conversion is more in the presence of the fluoride ion with more water structure making ability, as represented in the Hofmeister series. The viscosity of the copolymer solutions remains practically constant upon addition of chloride salts but shows an increasing trend in the presence of fluoride ion salts at high copolymer concentration. It has also been shown that ethanol with a strong affinity toward both the core and corona

\* Corresponding author. E-mail: rajibg@barc.gov.in, rajugang@yahoo.co.in. Phone: +91-22-25590286. Fax: +91-22-25505150.

<sup>†</sup> V.N. South Gujarat University.

<sup>‡</sup> Chemistry Division, Bhabha Atomic Research Center.

<sup>§</sup> Radiation & Photochemistry Division, Bhabha Atomic Research Center.

<sup>||</sup> Solid State Physics Division, Bhabha Atomic Research Center.

induces a simultaneous increase in micellar size and viscosity at room temperature, which is otherwise not observed in the presence of water structure making  $\text{Cl}^-$  ions.<sup>22,23</sup> These results suggest that the rearrangement and growth of the P123 micelles induced by the water structure making anions are kinetically restricted, and the rate of them is enhanced in the presence of a core loving solvent. A study on the dynamics of the aggregation of the block copolymer in the aqueous medium also suggests that the relaxation process associated with the micellar restructuring slows down significantly with an increase in the molecular weight of the copolymer and also has an activation barrier associated with it.<sup>20</sup> The observed time dependent growth of the P123 micelles probably is due to the higher molecular weight of P123 as compared to those pluronics which show sphere-to-rod micellar growth in the aqueous medium. Whereas the influence of ethanol in modulating the growth rate of the P123 micelles through its interaction with the micellar core has been studied, the role of additives that modulate the micellar dehydration process, a factor that is known to be responsible for sphere-to-rod shape transition of the pluronic micelles,<sup>17</sup> is not understood yet. In view of these, we have carried out a systematic study of the time dependent sphere-to-rod growth characteristics of the pluronic micelles in the aqueous medium as a function of the water structure making abilities of the anions. The role of ethanol in improving the growth characteristics of the copolymer micelles has also been elucidated on the basis of our spectroscopic studies.

## Experiments

**Materials and Sample Preparation.** The triblock copolymers Pluronic P123, P103, P105, P85, P104, F127, and L64 were procured from BASF Corp., Parsippany, NJ. Sodium chloride was purchased from Merck, India, sodium phosphate and sodium fluoride were purchased from SD. Fine.-Chem limited, India, and pyrene was obtained from Baker Chemical Co., New Jersey. The copolymer solutions with different salt and ethanol concentrations were prepared by weighing required amounts of water, copolymer, salt, and ethanol and keeping them in a refrigerator in tightly closed glass stoppered vials for about 1 week.

**Methods. Viscometry.** The absolute viscosities of the solutions at different temperatures were measured by using calibrated Cannon Ubbelohde viscometers<sup>25</sup> in a temperature controlled water bath.

**Dynamic Light Scattering (DLS).** DLS measurements of the solutions were performed using a Malvern 4800 Autosizer employing a 7132 digital correlator. The light source was an argon ion laser operated at 514.5 nm with a maximum output power of 2 W. The average decay rate was obtained by analyzing the electric field autocorrelation function  $g^1(\tau)$  vs time data using a modified cumulants method or a stretched biexponential equation.<sup>26–29</sup> The modified cumulants method overcomes the limitations of cumulants analysis to fit the data at long correlation time or large polydispersity.<sup>30</sup> The changes in the refractive index and the viscosity of water upon addition of salt were taken into account while analyzing the correlation function data. The apparent equivalent hydrodynamic radii of the micelles were calculated using the Stokes–Einstein relationship. For anisotropic micelles, the lengths of the micelles were estimated from the translational diffusion coefficient employing Perrin's formula. For prolate ellipsoids, the diffusion coefficient ( $D$ ) is related to the axial ratio ( $\rho$ ) and semimajor axis ( $a$ ) of the micelles, by the relation<sup>31</sup>

$$D = kT[G(\rho)]/6\pi\eta a$$

$$G(\rho) = (1 - \rho^2)^{-1/2} \ln\{[1 + (1 - \rho^2)^{1/2}]/\rho\} \quad (1)$$

where  $D$  is the translational diffusion coefficient,  $\rho$  is the ratio of the semiminor axis to the semimajor axis with a value of  $<1$ , and  $\eta$  is the viscosity of the medium. The semiminor axis is fixed as the radius of the spherical micelle before the onset of growth.

**Small Angle Neutron Scattering (SANS).** SANS measurements were carried out on the samples prepared in  $\text{D}_2\text{O}$  at the SANS facility at DHRUVA reactor, Trombay. The mean incident wavelength was 5.2 Å with  $\Delta\lambda/\lambda = 15\%$ . The scattering was measured in the scattering vector ( $q$ ) range of 0.017–0.3 Å<sup>−1</sup>. The measured SANS data were corrected for the background, the empty cell contributions, and the transmission and were placed on an absolute scale using standard protocols. Correction due to the instrumental smearing was taken into account throughout the data analysis.<sup>32</sup>

The differential scattering cross section per unit volume ( $d\Sigma/d\Omega$ ) of monodisperse micelles can be written as<sup>33,34</sup>

$$d\Sigma/d\Omega = NF_{\text{mic}}(q)S(q) + B \quad (2)$$

$N$  is the number density of the micelles and  $B$  is a constant term that represents the incoherent background scattering mainly from the hydrogen atoms present in the sample.  $F_{\text{mic}}(q)$  is the form factor characteristic of specific size and shape of the scatterers, and  $S(q)$  is the structure factor that accounts for the interparticle interaction. The block copolymer micelles can be considered as a core–shell particle with different scattering length densities of the core and the shell. The structure of these micelles is described using a model consisting of PEO chains attached to the surface of the PPO core.<sup>33,34</sup> The form factors for spherical and ellipsoidal micelles were used as formulated by Pedersen.<sup>33</sup> In this model, the shell is described as consisting of noninteracting Gaussian polymer chains and these chains are assumed displaced from the core (or else the mathematical approximations will not work, as the chains overlap each other and the core); i.e., a mushroom polymer configuration is assumed. Nonpenetration of the chains into the core region is mimicked by moving the center of mass of the chains by a distance  $R_g$  away from the surface of the core, where  $R_g$  is the radius of gyration of the chains. The form factor of the micelles  $F_{\text{mic}}(q)$  comprises four terms: the self-correlation of the core, the self-correlation of the chains, the cross term between the core and chains, and the cross term between different chains. The interparticle structure factor  $S(q)$  for block copolymer micelles is usually captured by the analytical solution of the Ornstein–Zernike equation with the Percus–Yevick approximation,<sup>35</sup> employing hard sphere interaction, but since the present work is carried out at low concentration, this term is not included in the analysis of the data.

In the case of polydisperse micelles, the equation can be written as

$$d\Sigma/d\Omega(q) = \int d\Sigma/d\Omega(q, R_c)f(R_c)dR_c + B \quad (3)$$

The polydispersity in the micellar size ( $R = R_c$ ) has been accounted for by a Schultz distribution, as given by the equation

$$f(R_c) = [(z + 1)/R_{\text{cm}}]^{z+1} R_c^z \exp[-(z + 1)/R_{\text{cm}}R_c] [1/(\Gamma(z + 1))] \quad (4)$$

where  $R_{\text{cm}}$  is the mean value of the distribution and  $z$  is the width parameter. The polydispersity of this distribution is given by  $\Delta R_c/R_{\text{cm}} = 1/(z + 1)^{1/2}$ .

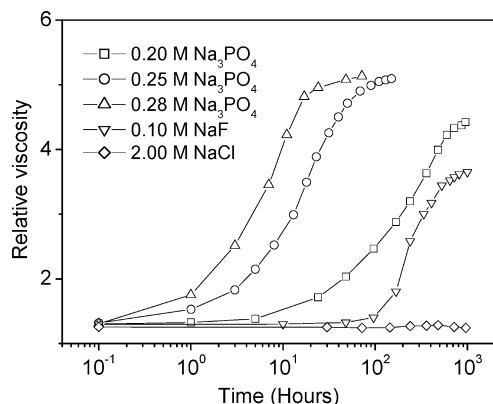


**Figure 1.** Relative viscosity ( $\eta_{\text{rel}}$ ) vs time plots of 1% P123 solutions recorded at 30 °C in the presence of different salts.

**Steady-State Fluorescence Studies.** Steady-state fluorescence spectra of pyrene were recorded using a Hitachi (Tokyo, Japan) model F-4500 spectrofluorimeter. Pyrene has been extensively used as a fluorescence probe to investigate the formation of hydrophobic microdomains by surfactants and copolymers. In particular, the pyrene spectrum shows several vibronic peaks, and the ratio of the intensities of the third and first vibronic peak (i.e.,  $I_3/I_1$ ) is a sensitive indicator of the polarity of the pyrene microenvironment.<sup>36,37</sup> The excitation wavelength was 335 nm, and the emission spectra were recorded from 350 to 450 nm.

## Results and Discussion

**Viscometry.** The room temperature viscosities of the aqueous pluronic solutions are determined primarily by the concentration and shape of the pluronic micelles. The fact that the intermicellar interaction is repulsive or weakly attractive in nature plays an insignificant role in it, especially at low copolymer concentration.<sup>19</sup> In Figure 1, we have shown the time dependence of the viscosity of the 1% P123 solutions at 30 °C in the presence of NaCl, NaF, and Na<sub>3</sub>PO<sub>4</sub>. P123 solutions show time dependent sphere-to-rod micellar shape transition on approaching their cloud points, and the presence of these salts is expected to reduce the micellar shape transition temperature down to room temperature.<sup>22–24</sup> The viscosity of the copolymer solutions does not show any increasing trend over a few weeks time up to a concentration of 2 M NaCl or even higher. In the case of NaF, it increases slowly over the same time period at 1 M concentration. NaF concentration below this (up to 0.8 M) does not lead to any significant increase in viscosity with time, and above this concentration, the copolymer solutions undergo phase separation. The situation is very different in the case of Na<sub>3</sub>PO<sub>4</sub>, as the rates of increase in viscosity are found to be significantly higher than that observed in the presence of 1 M NaF. In the literature, the observed time dependent increase in viscosity at a fixed copolymer concentration are attributed to sphere-to-rod micellar shape transition.<sup>21–23</sup> Our DLS studies shown in the next section suggest that in the present case too the observed increase in the viscosity of the copolymer solutions is accompanied by a sphere-to-rod growth of the micelles present. As observed in the case of Na<sub>3</sub>PO<sub>4</sub>, the growth rate is a function of salt concentration, as it decreases quite significantly with a decrease in the Na<sub>3</sub>PO<sub>4</sub> concentration from 0.28 to 0.2 M. The observed time dependent micellar growth and the phase separation in the aqueous P123 solutions can be attributed to slow micellar restructuring essential to attain the equilibrium micellar structure in the presence of the water structure making ions.<sup>20,21</sup>

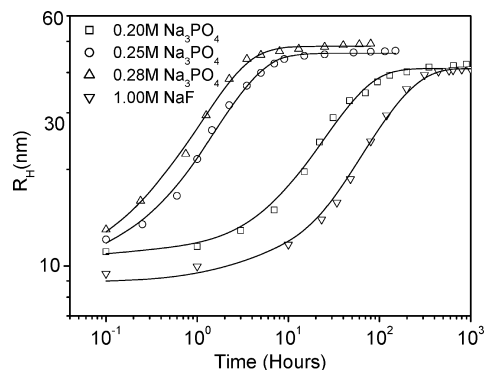


**Figure 2.** Hydrodynamic size ( $R_h$ ) vs time plots of 1% P123 solution recorded at 30 °C in the presence of different salts. The solid lines represent fits to the data.

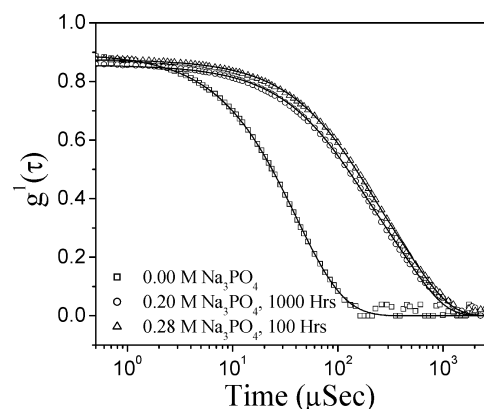


**Figure 3.** Correlation function diagrams of 1% P123 solutions recorded at 30 and 130° scattering angle as a function of salt concentration. The solid lines represent fits to the data.

A large aggregation number of the micelles, principally because of the highly hydrophobic nature of the copolymer molecules, and a large molecular weight of the copolymer could be the reasons behind the observed slow restructuring of the P123 micelles.<sup>20</sup> The observed results clearly show that such micellar restructuring leading to the sphere-to-rod shape transition of the copolymer micelles becomes faster with an increase in the water structure making ability of the anions in the order  $\text{Cl}^- < \text{F}^- < (\text{PO}_4)^{3-}$ , as conceptualized in the Hofmeister series. In the literature, the sphere-to-rod transition of the pluronic micelles with an increase in temperature has been attributed to the dehydration of the micellar corona region with a decrease in the solubility of the PEO blocks.<sup>17</sup> Our results thus suggest that the rate of such dehydration and hence the rate of restructuring and growth of the copolymer micelles increases with an increase in the structure making ability of the anions. Further insight into the observed micellar growth characteristics has been given by the DLS results discussed in the next section.

**Dynamic Light Scattering Studies.** DLS studies on the effect of salts on the 1% copolymer solution are shown in Figures 2 and 3. Figure 2 shows that the observed increase in viscosity with time in the presence of salt is accompanied by a time dependent increase in the micellar size. For each copolymer solution, the micellar size starts increasing earlier than their respective relative viscosities shown in Figure 1. The reason for this is that at low copolymer concentration the viscosities of the copolymer solutions start increasing only after the copolymer micelles reach a sufficiently high aspect ratio to attain a rodlike shape. The observed increase in the micellar size with time is signified by a shift in the correlation function vs time plots to longer time scale, as shown in Figure 3. These



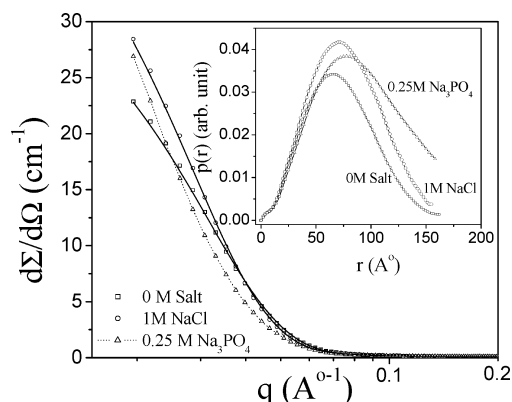
**TABLE 1: Hydrodynamic Radius ( $R_h$ ), the Polydispersity Index (PI), the Rod Length ( $L$ ), the Relaxation Time for the Correlation Function ( $\tau_s$ ), the Stretching Exponent ( $\beta$ ), and the Relaxation Time ( $\tau_r$ ) of the Growth Process of the P123 Micelles at 30 °C**

salt concentration	$R_h$ (nm)	PI	rod length ( $L$ ) (nm)	$\tau_s$ ( $\mu$ s)	$\beta$	$\tau_r$ (h)
1% P123, 0.00 M salt	9.4	0.08				
1% P123, 1.00 M NaF	40.94	0.40	277.6			122.0
1% P123, 0.20 M $\text{Na}_3\text{PO}_4$	42.42	0.38	289.2			38.1
5% P123, 0.20 M $\text{Na}_3\text{PO}_4$	30.21			357	0.74	
10% P123, 0.20 M $\text{Na}_3\text{PO}_4$	26.50			625	0.53	
1% P123, 0.20 M $\text{Na}_3\text{PO}_4$ with 1.5% ethanol	43.5	0.42	301.2			6.3
1% P123, 0.20 M $\text{Na}_3\text{PO}_4$ with 3.0% ethanol	44.74	0.38	311.7			3.4
1% P123, 0.25 M $\text{Na}_3\text{PO}_4$	46.8	0.39	330.7			2.7
1% P123, 0.28 M $\text{Na}_3\text{PO}_4$	49.2	0.44	357.8			1.8
1% P123, 0.28 M $\text{Na}_3\text{PO}_4$ , 10 times diluted	38.2	0.35	251.4			

copolymer micelles are known to undergo a sphere-to-rod transition when the core diameter of the micelle reaches the maximum length of the PPO block. In the present case, the micellar hydrodynamic radius reaches as high as about 49 nm (Table 1), which is much more than the combined length of the PPO and PEO blocks. This and the accompanied viscosity enhancement suggest that the copolymer micelles undergo a sphere-to-rod shape transition. The observed micellar growth is also accompanied by a large increase in the polydispersity of the micelles due to the presence of spherical micelles along with the majority amount of wormlike micelles.<sup>29</sup> To accommodate this enhanced polydispersity, the correlation function data were analyzed on the basis of the modified cumulants method.<sup>26</sup> The hydrodynamic sizes of the micelles thus obtained were used to calculate the length of the rodlike micelles using Perrin's formula. Denkova et al.<sup>23</sup> studied the time constants of the process of growth of P123 micelles as a function of ethanol concentration based on the equation represented as

$$R_H(t) = R_{H,\text{eq}} + (R_{H,0} - R_{H,\text{eq}}) \exp(-t/\tau_r)$$

where  $R_{H,\text{eq}}$  is the equilibrium or final size,  $R_{H,0}$  is the initial size, and  $\tau_r$  is the relaxation time of the growth process. Analysis of our data based on this equation shows (Table 1) that the relaxation time increases as the growth process slows down with variation in the salt concentration and the salt type. The analysis, however, fails to explain the time dependence of the viscosity of the copolymer solution at higher time scale. The fitted data show a saturation of the micellar size when the micellar size obtained as well as the viscosities of the copolymer solutions continues to increase with time (Figures 1 and 2).

**Figure 4.** SANS patterns of 1% aqueous copolymer solutions at 30 °C as a function of salt concentration. The solid lines represent fits to the data using spherical form factors for 0 and 1 M NaCl. The corresponding pair distance distribution function [ $p(r)$ ] plots are shown in the inset.**TABLE 2: Core Radius ( $R_c$ ), Aggregation Number ( $N_{\text{agg}}$ ), and Polydispersity ( $\Delta R_c/R_{\text{cm}}$ ) of the Micelles in 1% P123 Solutions at 30 °C<sup>a</sup>**

NaCl conc. (M/L)	$R_c$ (nm)	$N_{\text{agg}}$	$\Delta R_c/R_{\text{cm}}$ (%)
0.0 M NaCl	$5.32 \pm 0.05$	94	$20.8 \pm 0.4$
1.0 M NaCl	$5.77 \pm 0.02$	120	$12.2 \pm 0.2$

<sup>a</sup> The radius of gyration of the chains ( $R_g$ ) was kept fixed at 1.2 nm as reported earlier.<sup>44</sup>

**SANS Studies.** Additional confirmation about the variation in the growth characteristics of the P123 micelles in the presence of different salts could be obtained from SANS studies shown in Figure 4. A significant shift in the SANS plot to lower " $q$ " region in the presence of 0.25 M  $\text{Na}_3\text{PO}_4$  is suggestive of a significantly higher growth of the micelles as compared to that observed in the presence of 1 M NaCl. We, however, could not calculate the size of the rodlike micelles obtained in the presence of 0.25 M  $\text{Na}_3\text{PO}_4$ , because of our limited  $q$  region of measurement. An accurate estimation of the size of these micelles will require SANS measurement down to much lower  $q$  values that could not be obtained in our instrument. The micellar parameters obtained from the analysis of the data for the other two are shown in Table 2. As expected, the core radius and the corresponding aggregation number of the spherical P123 micelles increase in the presence of 1 M NaCl. The polydispersity index of the micelles, on the other hand, decreases upon addition of NaCl, which bears a resemblance to the effect of enhancement in the temperature of the pluronic solutions.<sup>13</sup> To understand the micellar structure, we calculated the pair distance distribution function [ $p(r)$ ] data for these plots obtained using the program GENOM made by Svergun and A. Semenyuk.<sup>38,39</sup> As shown in the inset of Figure 4, a significantly higher asymmetry in the  $p(r)$  plot in the presence of 0.25 M  $\text{Na}_3\text{PO}_4$  is a clear signature of the presence of higher anisotropy of the micelles in the form of a rodlike shape.

**The Effect of Ethanol.** Ethanol, being a good solvent for both the core and the corona, reduces the CMC, CMT, and sphere-to-rod transition temperature.<sup>40–42</sup> Its presence thus is expected to suppress the sphere-to-rod growth behavior of the copolymer micelles. We, however, observed that the presence of ethanol leads to a significant improvement in the micellar growth rate. This is shown in Figure 5 where the plots of variations of micellar size and the viscosities of the copolymer solutions as a function of time in the presence of 0.2 M  $\text{Na}_3\text{PO}_4$  with 1.5 and 3% ethanol are shown. The figure shows that the presence of ethanol leads to a significant enhancement in the rate of micellar growth (Table 1) and the viscosity enhancement. These results are in agreement with the literature report that ethanol induces room temperature sphere-to-rod micellar growth, which is otherwise suppressed in the presence of 2 M KCl.<sup>23</sup> It

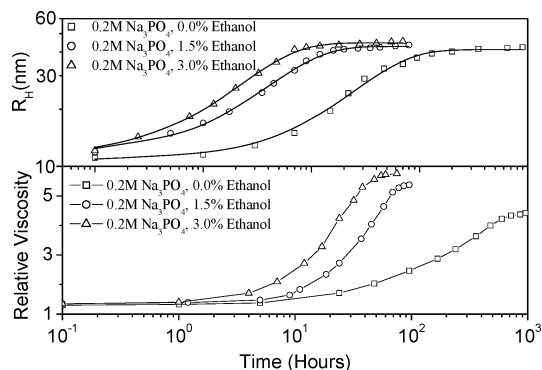


**Figure 5.** Hydrodynamic size ( $R_h$ ) and relative viscosity ( $\eta_{rel}$ ) vs time plots of 1% P123 solution in the presence of 0.2 M  $\text{Na}_3\text{PO}_4$  with 1.5 and 3% ethanol.

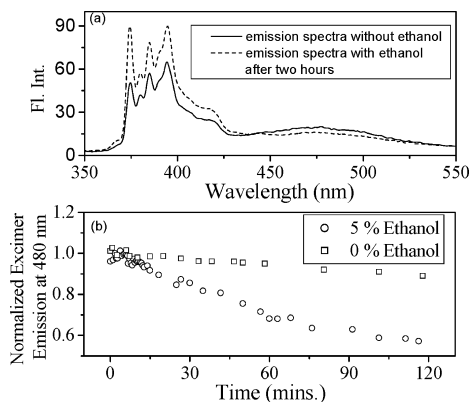


**Figure 6.** (a) Fluorescence spectra of pyrene in 5% P123 solution without ethanol (solid) and with ethanol after 2 h (dashed). (b) The decrease in the normalized excimer emission intensity at 480 nm with time due to solute exchange. The kinetics of solute exchange is faster in the presence of ethanol.

has been suggested that the observed enhancement in the growth rate of the micelles in the presence of ethanol occurs due to the swelling of the micellar core by ethanol, which facilitates the otherwise slow micellar restructuring process.<sup>22,23</sup> To shed further light on this aspect, we have carried out fluorescence measurements on the P123 solutions and studied the behavior of solute (pyrene) exchange kinetics by a change in the excimer fluorescence emission (higher wavelength 480 nm band) intensity in the absence and presence of ethanol. The concentration of pyrene was kept such that the average occupancy of a solute per P123 micelle is just above 2, so that we observe the excimer fluorescence along with dominant monomer emission. Treating this solution with an excess of empty micelles (nearly half dilution in our case) results in exchange of probes between the micelles, which in turn leads to a decrease in excimer emission intensity and a concomitant increase in the monomer emission at lower wavelengths as a function of time. This experiment has also been repeated in the presence of 5% ethanol. The results of this solute exchange, i.e., pyrene spectra and the traces for the pyrene excimer emission, are shown in Figure 6, which clearly indicate that the exchange of the probe becomes significantly faster in the presence of 5% ethanol.

In the literature, solute exchange has been explained on the basis of either exit and reentry, or two different pathways involving the micelles, namely, fission of a micelle into two submicelles, which subsequently grow back to, i.e., normal micelles, or fusion of two micelles to form a short-lived “super-micelle”, which rapidly fragments back to two normal micelles.<sup>43–47</sup> Studies on the pluronics suggest that the micellar

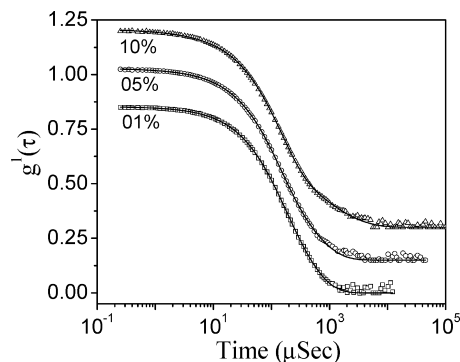


**Figure 7.** Correlation function diagrams of the copolymer solutions recorded at 30 and 130° scattering angle as a function of P123 concentration. The plots are shifted vertically with an increase in the P123 concentration, and the solid lines represent fits to the data.

restructuring occurs through inter-micellar collisions and subsequent micellar disintegration,<sup>20,46,47</sup> which is quite similar to the second pathway for the pyrene exchange processes mentioned above. The present observations, however, do not throw light on the mechanism behind the faster pyrene exchange process in the presence of ethanol due to the reason that pyrene entry and exit time in the micellar system is likely to be of the order of milliseconds, which is incidentally much faster than the observed rate of decrease of the normalized excimer emission intensity.<sup>43–45</sup> Clearly, further studies are necessary to understand the present system in the light of the existing theories. Using hydrophobically modified pyrene derivatives, like PyC8, PyC12, and Py-triglyceride, with much lower solubility in water as compared to pyrene could be considered as one of the options, as they can effectively thwart the exit and re-entry mechanism.<sup>43</sup> Nevertheless, the observed faster decrease in the excimer emission intensity with time in the presence of ethanol suggests that the solvent has a significant influence on the process of restructuring and growth of the pluronic micelles. Ethanol is known to be a good solvent for both the PEO and PPO block and it prefers to stay within the micelles because of its difference in the dielectric constant value with that of water.<sup>48</sup> Since the enhanced solvation in the corona will not favor a sphere-to-rod micellar shape transition, a solvated core in the presence of ethanol probably facilitates a faster exchange of unimers between the micelles and a subsequent faster micellar growth. These results thus suggest that, in addition to the ability of the anions to dehydrate the micellar corona, solvation characteristics of the micellar core also play an important role in determining the sphere-to-rod growth characteristics of the pluronic micelles.

**The Effect of Copolymer Concentration.** To shed further light on this system, DLS studies were carried out on the salt induced micellar growth as a function of copolymer concentration. The results shown in Figure 7 illustrate that the nature of the correlation function changes from the single exponential to biexponential form with an increase in the copolymer concentration. The data for the 5 and 10% P123 solution in the presence of 0.2 M  $\text{Na}_3\text{PO}_4$  thus can be best fitted on the basis of a stretched biexponential equation represented as follows

$$g^{(1)}(t) = A_f \exp(-t/\tau_f) + A_s \exp[(-t/\tau_s)^\beta] \quad (5)$$

where  $A_f$  and  $A_s$  are the amplitudes for the fast and slow relaxation modes corresponding to the relaxation times  $\tau_f$  and  $\tau_s$ , respectively.<sup>27–29</sup> The relaxation time for the fast mode is associated with the diffusion of the rodlike micelles, and that of the slow mode can be ascribed to coupling between

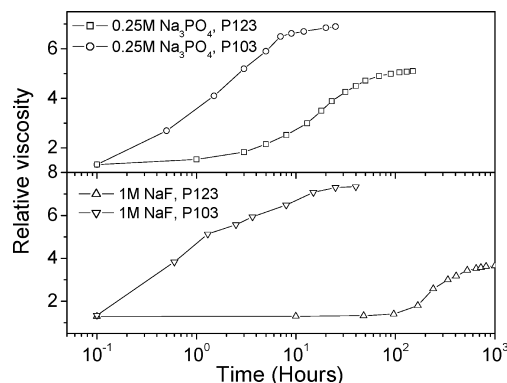


**Figure 8.** Comparison of the relative viscosity ( $\eta_{rel}$ ) vs time plots of 1% P123 and 1% P103 solutions recorded at 30 °C in the presence of 0.25 M  $\text{Na}_3\text{PO}_4$  and 1 M NaF.

concentration fluctuation and stress relaxation in entangled rodlike micelles. According to the coupling theory for the entangled rodlike systems, the exponent  $\beta$  ( $0 < \beta \leq 1$ ) is inversely proportional to the width of the distribution of the relaxation times of the slow mode, and an increase in the micellar entanglement will lead to the observation of an increase in  $\tau_s$  and a decrease in  $\beta$ .<sup>27,28</sup> Table 1 shows an increase in the concentration of the micelles due to an increase in the copolymer concentration indeed leads to an increase in  $\tau_s$  and a decrease in  $\beta$ . These results thus also suggest that the observed enhancement in the viscosity of the copolymer solution in the presence of salt is due to the formation of rodlike micelles.

**The Effect of Copolymer Composition.** In an effort to understand the effect of copolymer composition on the time dependent growth behavior of the copolymer micelles, we explored a number of copolymers, namely, F127 (MW 12600, PPO wt % 30), P85 (MW 4600, PPO wt % 50), P105 (MW 6500, PPO wt % 50), P104 (MW 5600, PPO wt % 57), P103 (MW 4900, PPO wt % 69), and L64 (MW 2900, PPO wt % 60), but observed similar kinetically restricted growth behavior in the presence of salts only in P103. P85 and L64 show sphere-to-rod micellar shape transitions, which are fast compared to the time scale of viscosity and DLS measurements, but the other copolymers do not show any such micellar shape transition because of their hydrophilic character. Both P123 and P103 are highly hydrophobic (PPO weight fraction  $\approx 70\%$ ) and have a reasonably high molecular weight, which make them suitable candidates for the restricted restructuring and growth of their micelles. Comparisons of the time dependence of the viscosity of the 1% P103 and 1% P123 solutions in the presence of the 1 M NaF and 0.25 M  $\text{Na}_3\text{PO}_4$  are shown in Figure 8. Like in the case of P123, no change in the viscosity of the 1% P103 solution could be induced in the presence of 2 M NaCl. However, the rates of viscosity enhancement in the presence of  $\text{Na}_3\text{PO}_4$  and NaF have been found to be significantly higher in the P103 solutions than in the P123 solutions. These results thus suggest that, although these two copolymers have comparable PPO weight fraction, a lower molecular weight of P103 favors a faster micellar restructuring and growth process than that observed in the case of P123. The observed growth rate of the P103 micelles is found to be slower than their rate of restructuring by about 1 order.<sup>47</sup> This discrepancy could be due to the presence of additional kinetics involved in the dehydration of the micellar corona by the anions present in our system.

**The Stability of the Wormlike Micelles.** In order to check whether the room temperature wormlike micelles formed in the presence of salts are kinetically stable or not, we have subjected the 1% solution with 0.28 M  $\text{Na}_3\text{PO}_4$  to 10 times dilution and

kept it at room temperature (30 °C) for 1 week's time. Since at this dilution the  $\text{Na}_3\text{PO}_4$  concentration present (0.028 M) is insufficient to support the wormlike structure of the micelles, the micelles should become smaller in size to get back to their spherical shape. Our DLS studies, however, show that not only the size of the micelles does not change significantly upon dilution, but it also remains practically constant with respect to time. This is reflected in the comparison of the hydrodynamic radius of the micelle in 1% solution and that of the diluted one after 1 week given in Table 1. The practically unchanged correlation function plot and close values of the micellar size suggest that the wormlike micelles formed in the presence of salts have significant kinetic stability with respect to dilution. According to recent reports, flexible wormlike micelles of bioinert copolymers are potential controlled drug release systems because of their penetrating ability into the body tissues and their minimum adhesion in flow to the cells in human blood.<sup>49</sup> In view of this, and the influence of the micellar disintegration on drug discharge behavior upon dilution within the human body,<sup>50,51</sup> the observed kinetic stability of the wormlike P123 micelles can have an important bearing on the applications of pluronics as drug delivery systems.

## Conclusion

The sphere-to-rod growth characteristics of the Pluronics P103 and P123 have been studied in the presence of salts containing different water structure making anions. Both of these copolymers show time dependent micellar growth with the growth rate decreasing quite remarkably with a decrease in the water structure making ability of the anions in the order  $(\text{PO}_4)^{3-} > \text{F}^- > \text{Cl}^-$ . The observed time dependent micellar growth in these systems is attributed to the slow restructuring process of the copolymer micelles arising due to the large molecular weight of P103 and P123. It has been suggested that the enhancement in the micellar growth rate with increasing water structure making ability of the anions results due to an increasing rate of dehydration of the corona of the copolymer micelles. A remarkable increase in the micellar growth rate is also brought about by the addition of ethanol, which has been attributed to an enhanced rate of micellar restructuring process in the presence of a more labile core swelled by ethanol. These results thus show how the core and the corona solvation characteristics of the pluronic micelles play important roles in determining their restructuring and growth characteristics. Finally, the observation of a higher micellar growth rate for the smaller molecular weight copolymer P103 suggests that the entanglements of the copolymer unimers within the micelles too determine the restructuring and growth characteristics of the copolymer micelles in a significant way.

## References and Notes

- (1) Chu, B. *Langmuir* **1995**, *11*, 414.
- (2) Wanka, G.; Hoffmann, H.; Ulbricht, W. *Macromolecules* **1994**, *27*, 4145.
- (3) Hurter, P. N.; Hatton, T. A. *Langmuir* **1992**, *8*, 1291.
- (4) Schmolka, I. R. *J. Am. Oil Chem. Soc.* **1977**, *54*, 110.
- (5) Pandit, N. K.; Wang, D. *Int. J. Pharm.* **1998**, 167183.
- (6) Zhang, K.; Khan, A. *Macromolecules* **1995**, *28*, 3807.
- (7) Hvidt, S.; Jorgensen, E. B.; Brown, W.; Schillen, K. *J. Phys. Chem.* **1994**, *98*, 12320.
- (8) Mortensen, K.; Brown, W.; Norden, B. *Phys. Rev. Lett.* **1992**, *68*, 2340.
- (9) Malmsten, M.; Lindman, B. *Macromolecules* **1992**, *25*, 1282.
- (10) Alexandridis, P.; Holzwarth, J. F.; Hatton, T. A. *Macromolecules* **1994**, *27*, 2414.
- (11) Wanka, G.; Hoffmann, H.; Ulbricht, W. *Colloid Polym. Sci.* **1990**, *268*, 101.

- (12) Glatter, O.; Scherf, G.; Schillen, K.; Brown, W. *Macromolecules* **1994**, *27*, 6046.
- (13) Brown, W.; Schillen, K.; Almgren, M.; Hvidt, S.; Bahadur, P. *J. Phys. Chem.* **1991**, *95*, 1850.
- (14) Al-saden, A. A.; Whateley, T. L.; Florence, A. T. *J. Colloid Interface Sci.* **1982**, *90*, 303.
- (15) Zhou, Z.; Chu, B. *J. Colloid Interface Sci.* **1988**, *126*, 171.
- (16) Mortensen, K.; Pedersen, J. S. *Macromolecules* **1993**, *26*, 805.
- (17) Löf, D.; Niemiec, A.; Schillén, K.; Loh, W.; Olofsson, G. *J. Phys. Chem. B* **2007**, *111*, 5911.
- (18) Chen, W.-R.; Mallamace, F.; Glinka, C. J.; Fratini, E.; Chen, S.-H. *Phys. Rev. E* **2003**, *68*, 041402.
- (19) Ganguly, R.; Choudhury, N.; Aswal, V. K.; Hassan, P. A. *J. Phys. Chem. B* **2009**, *113*, 668.
- (20) Kositz, M. J.; Bohne, C.; Alexandridis, P.; Hatton, T. A.; Holzwarth, J. F. *Macromolecules* **1999**, *32*, 5539.
- (21) Ganguly, R.; Kumbhakar, M.; Aswal, V. K. *J. Phys. Chem. B* **2009**, *113*, 9441.
- (22) Denkova, A. G.; Mendes, E.; Coppens, M.-O. *J. Phys. Chem. B* **2008**, *112*, 793.
- (23) Denkova, A. G.; Mendes, E.; Coppens, M.-O. *J. Phys. Chem. B* **2009**, *113*, 989.
- (24) Alexandridis, P.; Holzwarth, J. F. *Langmuir* **1997**, *13*, 6074.
- (25) *ASTM Standard D 445-04 and D 446-04* **2004**, and the references within.
- (26) Hassan, P. A.; Kulshreshtha, S. K. *J. Colloid Interface Sci.* **2006**, *300*, 744.
- (27) Moitzi, C.; Freiberger, N.; Glatter, O. *J. Phys. Chem. B* **2005**, *109*, 16161.
- (28) Ngai, K. L. *Adv. Colloid Interface Sci.* **1996**, *64*, 1.
- (29) Ganguly, R.; Aswal, V. K.; Hassan, P. A. *J. Colloid Interface Sci.* **2007**, *315*, 693.
- (30) Koppel, D. E. *J. Chem. Phys.* **1972**, *57*, 4814.
- (31) Pecora, R. *Dynamic Light Scattering: Application of Photon Correlation Spectroscopy*; Plenum Press: New York, 1985.
- (32) Aswal, V. K.; Goyel, P. S. *Curr. Sci.* **2000**, *79*, 947.
- (33) Pedersen, J. S.; Gerstenberg, C. *Macromolecules* **1996**, *29*, 1363.
- (34) Pedersen, J. S. *J. Appl. Crystallogr.* **2000**, *33*, 637.
- (35) Percus, J. K.; Yevick, G. J. *Phys. Rev.* **1958**, *1*, 110.
- (36) Kalyansundaram, K. *Photochemistry in Microheterogeneous Systems*; Academic Press: Orlando, FL, 1987.
- (37) Lakowicz, J. R. *Principle of fluorescence spectroscopy*, 3rd ed.; Springer: New York, 2006.
- (38) Svergun, D. I.; Semenyuk, A. V.; Feigin, L. A. *Acta Crystallogr., Sect. A* **1988**, *44*, 244.
- (39) Svergun, D. I. *J. Appl. Crystallogr.* **1991**, *24*, 485.
- (40) Armstrong, J.; Chowdhry, B.; Mitchell, J.; Beezer, A.; Leharne, S. *J. Phys. Chem.* **1996**, *100*, 1738.
- (41) Ivanova, R.; Lindman, B.; Alexandridis, P. *Adv. Colloid Interface Sci.* **2001**, *89*, 351.
- (42) Ganguly, R.; Aswal, V. K.; Hassan, P. A.; Gopalakrishnan, I. K.; Yakhmi, J. V. *J. Phys. Chem. B* **2005**, *109*, 5653.
- (43) Rharbi, Y.; Li, M.; Winnik, M. A.; Hahn, K. G., Jr. *J. Am. Chem. Soc.* **2000**, *122*, 6242.
- (44) Rharbi, Y.; Li, M.; Winnik, M. A. *J. Phys. Chem. B* **2003**, *107*, 1491.
- (45) Almgren, M. *Chem. Phys. Lett.* **1980**, *71*, 539.
- (46) Almgren, M. *J. Am. Chem. Soc.* **1980**, *102*, 7882.
- (47) Michels, B.; Waton, G.; Zana, R. *Langmuir* **1997**, *13*, 3111.
- (48) Fernandez, V. V. A.; Soltero, J. F. A.; Puig, J. E.; Rharbi, Y. *J. Phys. Chem. B* **2009**, *113*, 3015.
- (49) Alexandridis, P.; Ivanova, R.; Lindman, B. *Langmuir* **2000**, *16*, 3676.
- (50) Kim, Y.; Dalhaimer, P.; Christian, D. A.; Discher, D. E. *Nanotechnology* **2005**, *16*, S484.
- (51) Pruitt, J. D.; Hussein, G.; Rapoport, N.; Pitt, W. G. *Macromolecules* **2000**, *33*, 9306.
- (52) Yang, T.-F.; Chen, C.-N.; Chen, M.-C.; Lai, C.-H.; Liang, H.-F.; Sung, H.-W. *Biomaterials* **2007**, *28*, 725.